Quantum Distributed Microgrid Control

Pouya Babahajiani, *Senior Member, IEEE,* Peng Zhang, *Senior Member, IEEE*
Department of Electrical and Computer Engineering, Stony Brook University, NY 11794, USA
pouya.babahajiani@stonybrook.edu, p.zhang@stonybrook.edu

***Abstract*—To empower flexible and scalable operations, distributed control of multi-inverter microgrids, based on classical communication networks among distributed energy resources, has attracted considerable attention. Notwithstanding this, resilience of the current schemes on classical communication makes microgrids vulnerable to cyber attacks. Inspired by quantum properties of quantum bits, in this paper, we devise a novel synchronization mechanism. We extend the synchronization framework utilized in distributed control algorithms to networks of quantum systems. By employing the architecture of quantum network, security of the protocol can be enhanced. Test results on two representative ac and dc microgrids validate the efficacy and universality of the quantum distributed control.**

***Index Terms*—Quantum distributed control, distributed frequency regulation, distributed voltage regulation.**

I. Introduction

Microgrids, featured by the autonomic coordination of their local energy sources and power demands, have proven to be a promising new paradigm of electricity resiliency, and thus their share in the energy sector is swiftly growing. To match up with the main characteristics of microgrids including flexibility and scalability, distributed control of multi-inverter microgrids has attracted considerable attention as it can achieve the combined goals of flexible plug-and-play architecture guaranteeing frequency and voltage regulation while preserving precise power sharing among nonidentical participating DERs [1].

With these in mind, microgrids have become a cyber-physical system that requires complicated network technologies to handle massive utilization of communication and computation devices, and it turns out that cybersecurity has emerged as a serious concern which has been extensively studied so as to mitigate data breach and improve security in smart grids [2]. However, the current power grids are going through a significant transformation such that the existing technology might not be adequate to address the security requirements.

On the other hand, the development of quantum computers will cause security break and they can easily make traditional methods of cryptography obsolete [3]. The supremacy and fast development of quantum schemes are paving the way for the realization of the quantum internet [4]. The concept of quantum internet is to make a new internet technology possible by enabling quantum communication between any two points. Several major applications have already been reported for quantum internet however, central to all these applications is the ability to transmit quantum bits (qubits) which cannot be copied, and any attempt to do so can be detected. This feature makes qubits well suited for security applications. Promising findings on quantum internet have even led some researchers to believe that all communications will eventually be done through quantum channels [5]. Inspired by these developments, we aim to devise a scalable quantum distributed controller that can guarantee synchronization.

Several efforts have been made to investigate consensus problems in the quantum domain. One existing approach is to model the quantum network's state evolution through the quantum synchronization master equation [6]. Another approach is to appeal to the gossip-type interaction between neighboring quantum computing devices [7]. However, in the existing approaches, measurement is not considered, i.e., the existing frameworks are valid as long as the corresponding quantum system is not measured, which makes them impractical for realistic distributed control of microgrids.

Motivated by the above challenges and potential to design a quantum synchronization scheme, in this paper we aim to develop a quantum distributed control framework to enable controlling networks of DERs through a network of quantum systems. To this end, we first formulate the quantum synchronization problem using a quantum master equation and characterize suitable jump operators to drive the quantum network to synchronization. The protocol we construct gives rise to a differential equation that allows analyzing the convergence. We utilize proper observables and show that all the corresponding expectations will eventually converge to a possibly time-varying target value, and finally exploit these expectation values as control signals to drive a network of DERs to synchronization.

II. Preliminaries

In this section, we introduce some fundamental concepts from quantum systems [8]. The (adjoint) † symbol indicates the transpose-conjugate in matrix representation, and the tensor product $\otimes$ is associated to the Kronecker product. The mathematical description of a single quantum system starts by considering a complex Hilbert space $\mathcal{H}$. We utilize Dirac's notation, where $|\psi\rangle$ denotes an element of $\mathcal{H}$, called a ket which is represented by a column vector, while $\langle\psi| = |\psi\rangle^\dagger$ is used for its dual, a bra, represented by a row vector, and $\langle\psi|\varphi\rangle$ for the associated inner product. We denote by I the identity operator. $[A, B] = AB - BA$ is the commutator and $\{A, B\} = AB + BA$ is the anticommutator of A and B.

Qubit, defined as the quantum state of a two-state quantum system, is the smallest unit of information, and it is analogous to classical bit. State of a qubit, represented by $|\psi\rangle = \alpha|0\rangle + \beta|1\rangle$, is superposition of the two orthogonal basis states $|0\rangle \sim [1,\ 0]^T$ and $|1\rangle \sim [0,\ 1]^T$. α and β are complex numbers in general, where $|\alpha|^2 + |\beta|^2 = 1$. We denote $|q_1\rangle \otimes ... \otimes |q_n\rangle \in \mathcal{H}^{\otimes n}$ as $|q_1...q_n\rangle$. In the case of mixed state, the state of a quantum

This work was supported in part by the US Department of Energy's Office of Electricity under Agreement No. 37533, in part by the US National Science Foundation under Grant Nos. ECCS-2018492, OIA-2134840 and OIA-2040599, and in part by Stony Brook University's Office of the Vice President for Research through a Quantum Information Science and Technology Seed Grant.

978-1-6654-0823-3/22/$31.00 ©2022 IEEE

system is represented by a *density operator* ρ, that is any self-adjoint positive semi-definite operator with trace one, and $\rho = |\psi\rangle\langle\psi|$ with $|\psi\rangle \in \mathcal{H}$ and $\langle\psi|\psi\rangle = 1$ are called pure states. For further information on qubits see [8], [9].

III. Quantum Distributed Control

We aim to construct a quantum distributed controller (QDC) to control a network of DERs. In this framework, each DER is equipped with or connected to a quantum computing (QC) device and then seeks a consensus among all the QCs in a distributed manner. The state of each quantum device can be described by a positive Hermitian density matrix ρ. Since synchronization requires interaction among all quantum devices, let us assume that each device can be considered as a quantum system and has access to the (quantum) information of its neighbors. The following Lindblad master equation is a suitable way to describe the dynamics of a system with dissipation:

$$\dot{\rho}(t) = -\frac{\imath}{\hbar}[H,\rho] + \sum_{i=1}^{n}\Big(C_i\rho C_i^{\dagger} - \frac{1}{2}\{C_i^{\dagger}C_i,\rho\}\Big), \tag{1}$$

where H is the effective Hamiltonian as a Hermitian operator over the underlying Hilbert space, $\hbar$ is the reduced Planck constant, $\imath$ denotes the imaginary unit, and C_i are jump operators. For more information on Markovian master equations in Lindblad form, see [10]. We demonstrate that utilizing suitable jump operators and observers for each quantum node would lead the average expectation values of all the observers to converge to a possibly time-varying target value and the synchronization rule follows the forced Kuramoto model.

A. Algorithm

Let us update the state of each quantum node at each time step as follows:

$$|q_i(t)\rangle = \begin{pmatrix} \cos\frac{\pi}{4} \\ e^{\imath\phi_i(t)}\sin\frac{\pi}{4}\end{pmatrix}, \qquad t \in \{0,1,2,\ldots\}, \tag{2}$$

which is the general state in polar coordinates set on the xy-plane, where $\phi_i(0) \in (0,\pi/2)$ and each $\phi_i(t)$, $t \geq 1$, is the averaged measurement outcome which can be obtained by simply averaging measurement outcomes of many realizations of a single experiment for node i.

Let $|\psi\rangle = |q_1q_2\cdots q_n\rangle$ be the state of the whole quantum network and $\rho = |\psi\rangle\langle\psi|$. We introduce the following master equation with unitary jump operators:

$$\dot{\rho}(t) = \sum_{i=1}^{n}(C_i\rho C_i^{\dagger} - \rho)dt + \sum_{\{i,j\}\in E}(C_{i,j}\rho C_{i,j}^{\dagger} - \rho)dt. \tag{3}$$

where $C_{i,j}$ is the swapping operator that specifies the external interaction between quantum computing devices i and j such that

$$\begin{aligned} &C_{i,j}(|q_1\rangle\otimes\ldots\otimes|q_i\rangle\otimes\ldots\otimes|q_j\rangle\otimes\ldots\otimes|q_n\rangle) \\ &\qquad = |q_1\rangle\otimes\ldots\otimes|q_j\rangle\otimes\ldots\otimes|q_i\rangle\otimes\ldots\otimes|q_n\rangle. \end{aligned} \tag{4}$$

where, $\otimes$ denotes the tensor product. Let us define the jump operator, C_i, by $C_i = I^{\otimes(i-1)}\otimes R_z(\phi)\otimes I^{\otimes(n-i)}$ with $R_z(\phi)$ being the rotation-Z operator which is a single-qubit rotation through angle ϕ radians around the Z-axis [9], where $\phi = \phi_{t,i} - \phi_i$. By definition, the operator C_i acts only on $|q_i\rangle$ without changing the states of other qubits. As can be seen, the jump operators C_i are state dependent and updated based on the target values $\phi_{i,t}$ and the measured $\phi_i(t)$. Therefore, at each time step, the master equation components are updated based on the target values and the obtained measurement signals. Thus, the density matrix at time $t+dt$ can be decomposed into $\rho(t+dt) = \rho(t) + d\rho_t$, where $d\rho(t)$ is defined in (3).

In order to obtain the angles ϕ_i, we introduce the following observables:

$$A_{1,i} = I^{\otimes(i-1)}\otimes\sigma_x\otimes I^{\otimes(n-i)}, \tag{5}$$
$$A_{2,i} = I^{\otimes(i-1)}\otimes\sigma_y\otimes I^{\otimes(n-i)}. \tag{6}$$

$A_{1,i}$ and $A_{2,i}$ act only on $|q_i\rangle$ where node-wise means, having σ_x and σ_y which are Pauli matrices [9] as observers at each node. The expectation value of an observable A in a state, represented by a density matrix ρ, is given by $\langle A\rangle = \mathrm{tr}(\rho\mathrm{A})$ [9].

For a general one qubit state ρ, $\mathrm{tr}(\rho\sigma_x) = r\sin\theta\cos\phi$, $\mathrm{tr}(\rho\sigma_y) = r\sin\theta\sin\phi$ and $\mathrm{tr}(\rho\sigma_z) = r\sin\theta$. Generally, Lindblad equation results in states becoming more mixed; however, we only let the system evolve in a short time and re-initialize the system in a product of pure qubit states. Therefore, we can consider $r = 1$ and $\theta = \pi/2$ and hence $\mathrm{tr}(\rho\sigma_{\mathrm{x}}) = \cos\phi_{\mathrm{i}}$, $\mathrm{tr}(\rho\sigma_{\mathrm{y}}) = \sin\phi_{\mathrm{i}}$, which are equivalent to $\mathrm{tr}(\rho\mathrm{A}_{1,\mathrm{i}}) = \cos\phi_{\mathrm{i}}$ and $\mathrm{tr}(\rho\mathrm{A}_{2,\mathrm{i}}) = \sin\phi_{\mathrm{i}}$, respectively. If we repeat the procedure of Lindblad evolution in a short duration, measurement and re-initialization, we can obtain approximated equations for ϕ_i's in the limit $dt \to 0$. The goal is to obtain the dynamic of the phase angles ϕ_i. Note that $\frac{d}{dt}\langle A\rangle = \frac{d}{dt}\mathrm{tr}(\rho\mathrm{A}) = \mathrm{tr}(\dot{\rho}\mathrm{A})$. From (3),

$$\begin{aligned} \mathrm{tr}(\dot{\rho}\mathrm{A}_{1,\mathrm{i}}) &= \cos\phi_{t,i} - \cos\phi_i + \sum_{j=1}^{n}a_{i,j}(\cos\phi_j - \cos\phi_i) \\ \mathrm{tr}(\dot{\rho}\mathrm{A}_{2,\mathrm{i}}) &= \sin\phi_{t,i} - \sin\phi_i + \sum_{j=1}^{n}a_{i,j}(\sin\phi_j - \sin\phi_i) \end{aligned} \tag{7}$$

where $a_{i,j} = 1$ if $C_{ij} \neq \mathbf{0}$ and $a_{i,j} = 0$ otherwise. Utilizing $\mathrm{tr}(\rho\mathrm{A}_{1,\mathrm{i}})$ and $\mathrm{tr}(\rho\mathrm{A}_{2,\mathrm{i}})$, we have the dynamic of ϕ_i as follows:

$$\begin{aligned} \dot{\phi}_i &= \frac{d}{dt}\arctan\left(\frac{\mathrm{tr}(\rho\mathrm{A}_{2,\mathrm{i}})}{\mathrm{tr}(\rho\mathrm{A}_{1,\mathrm{i}})}\right) \\ &= \left\{\frac{tr(\dot{\rho}A_{2,i})tr(\rho A_{1,i}) - tr(\dot{\rho}A_{1,i})tr(\rho A_{2,i})}{\cos^2\phi_i}\right\}\cos^2\phi_i \\ &= \sin(\phi_{t,i} - \phi_i) + \sum_{j=1}^{n}a_{i,j}\sin(\phi_j - \phi_i). \end{aligned} \tag{8}$$

It can be shown that, in (8) the pinning term $\sin(\phi_{t,i} - \phi_i)$ forces the phase ϕ_i to stick at the value $\phi_{t,i}$ and the coupling mechanism $\sum_{j=1}^{n}a_{i,j}\sin(\phi_j - \phi_i)$ helps to synchronize the entire system such that, all the nodes will synchronize to the pinner exponentially fast at a rate no less than μ, with μ being the following

$$\mu = \lambda_{\min}(\sigma_1 I + \sigma_2 BWB^T) > 0, \tag{9}$$

where, $\sigma_1 = \mathrm{sinc}(\varepsilon)$, $\sigma_2 = \mathrm{sinc}(2\varepsilon)$, $\mathrm{sinc(x)} \equiv \mathrm{sin(x)/x}$, $\varepsilon = \max_{1\leq i\leq n}|\zeta_i|$, ζ_i denotes the phase deviation of the ith oscillator from the pinner $\phi_{t,i}$, $W = \mathrm{diag}(\{a_{i,j}\}_{\{i,j\}\in E})$ is the diagonal matrix of edge weights and $B = [B_{i,j}]_{n\times m}$ is the incidence

978-1-6654-0823-3/22/$31.00 ©2022 IEEE

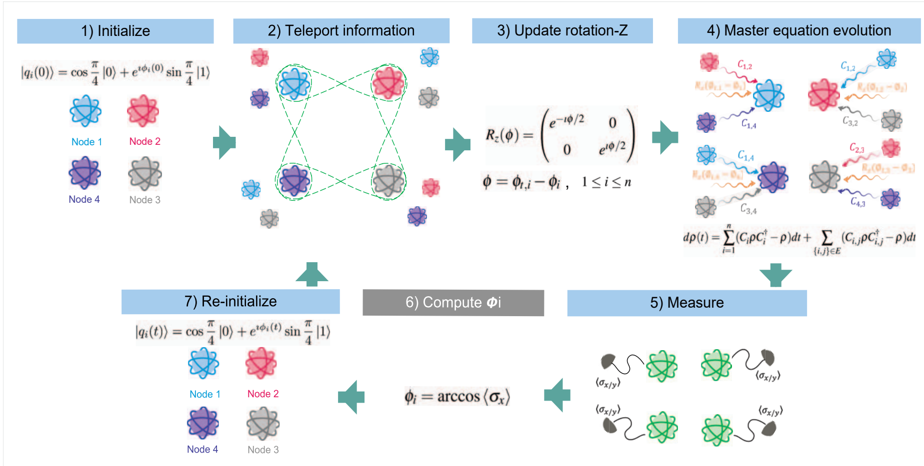

Fig. 1. Schematic depiction of the QDC.

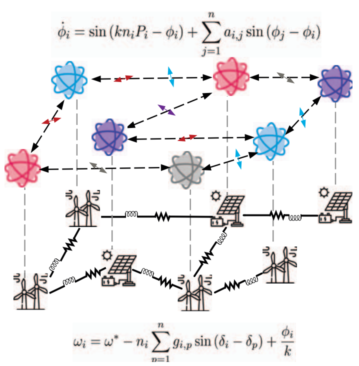

Fig. 2. Coupling of the physical microgrid to the network of quantum controllers can be considered as coupling of two Kuramoto models.

matrix of the communication graph G with m being the number of edges.

The basic outline of the algorithm is drawn schematically in Fig. 1 and is summarized as follows:

1) Initialize qubits as a point on the first quarter of the equator of the Bloch Sphere, i.e., $0 < \phi_i(0) < \pi/2$.
2) Teleport information throughout the network such that each quantum node receives the quantum information from its adjacent nodes.
3) At each node, update the rotation-Z (R_z) operator's argument based on the pinner ($\phi_{t,i}$) and the current value of the phase angle ϕ_i.
4) Evolve the master equation (3) for one time step δt by means of the swapping and rotation-Z operators.
5) Measure the expectation value of the σ_x or σ_y operator as the observer at each node. Repeating this multiple times and averaging gives the $\cos\phi_i$ or $\sin\phi_i$, depending on the exploited observable.
6) On classical hardware at each node, compute $\arccos\langle\sigma_x\rangle$ or $\arcsin\langle\sigma_y\rangle$ to obtain the phase angle ϕ_i.
7) Re-initialize the state of each quantum node
8) Go back to step 2.

IV. Quantum Distributed Controller for AC and DC Microgrids

A. Quantum Distributed Frequency Control

In AC microgrids, a predominantly inductive network naturally decouples the load sharing process; the reactive power regulator must handle the reactive load sharing by adjusting voltage magnitude while the active power regulator would handle the active load sharing through adjusting the frequency.

The locally deployed LC filter in each DER makes the output impedance inductive dominant [11], then the power sharing control laws that allow the active power to be shared based on DER units' rated capacities according to the droop setting, can be written as $\omega_i = \omega^* - n_iP_i$ where ω_i represents the frequency at DER$_i$, ω^* is a nominal network frequency, P_i is the measured active power injection at DER$_i$ and n_i is the gain of the droop coefficient. Here, we call n_iP_i the power sharing signal. Our developed QDC for AC microgrids is formulated as follows

$$\begin{aligned} \omega_i &= \omega^* - n_iP_i + \frac{\phi_i}{k}, \\ \dot{\phi}_i &= \sin(kn_iP_i - \phi_i) + \sum_{j=1}^{n} a_{i,j}\sin(\phi_j - \phi_i), \end{aligned} \tag{10}$$

where ϕ_i/k is the secondary control variable and the scaled power sharing signal, kn_iP_i, is the pinner. The power sharing signal is scaled to be restricted to $(0, \pi/2)$, thus, we select k such that $k < \frac{\pi/2}{\max(n_iP_i)}$. In a typical AC microgrid with distributed line impedances, since the susceptance of line impedance is usually much larger than its conductance, and also due to the small angle difference between each bus voltage, the output active power of each DER can be expressed as [12]

$$P_i = \sum_{p=1}^{n} E_iE_p|Y_{i,p}|\sin(\delta_i - \delta_p) = \sum_{p=1}^{n} g_{i,p}\sin(\delta_i - \delta_p) \tag{11}$$

where E_i is the nodal voltage magnitudes $E_i > 0$, $-Y_{i,p}$ is the admittance of the line between DER$_i$ and DER$_p$ and δ_i is the voltage phase angle.

From (11), the physical power network can be treated as a connected network whose entries of its adjacency matrix are $g_{i,p} = E_iE_p|Y_{i,p}|$ and hence, considering (10), it can be readily obtained that, the coupling of the network of quantum distributed controllers and the physical microgrid is the coupling of a forced Kuramoto model with a Kuramoto model (Fig. 2). At the steady state, the microgrid is assumed stable. Since the DERs' frequency must be equal, we have $\omega_i = \omega_j$ and thus $n_iP_i - \phi_i/k = n_jP_j - \phi_j/k \quad \forall i, j$. As mentioned before, ϕ_i

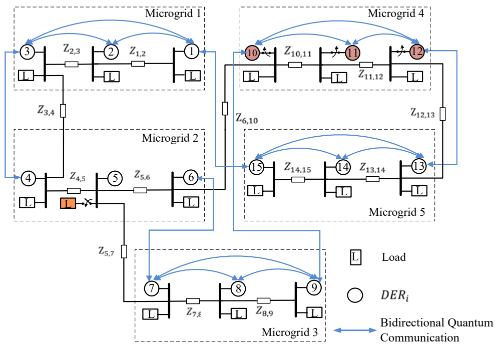

Parameter	Value	Parameter	Value
n_1, n_{13}	4×10^{-3}	n_2, n_{14}	4.5×10^{-3}
n_3, n_{15}	5×10^{-3}	n_4, n_7	10^{-3}
n_5, n_8	1.5×10^{-3}	n_6, n_9	2×10^{-3}
n_{10}	2.5×10^{-3}	n_{11}	3×10^{-3}
n_{12}	3.5×10^{-3}	Nominal frequency	60Hz
Nominal Voltage	380	Filter Capacitance	16μf
Filter Inductance	1.5mH	Output Impedance	1.5mH
$Z_{1,2}$, $Z_{4,5}$, $Z_{7,8}$, $Z_{10,11}$, $Z_{13,14}$	0.65Ω, 1.3mH	$Z_{2,3}$, $Z_{5,6}$, $Z_{8,9}, Z_{11,12}$, $Z_{14,15}$	0.5Ω, 1mH
$Z_{1,4}$, $Z_{5,7}$	0.35Ω, 1.8mH	$Z_{6,10}$	0.8Ω, 4mH
$Z_{12,13}$	0.7Ω, 2mH		

Fig. 3. Networked AC microgrids diagram and parameters - Blue bidirectional arrows represent the undirected quantum communications.

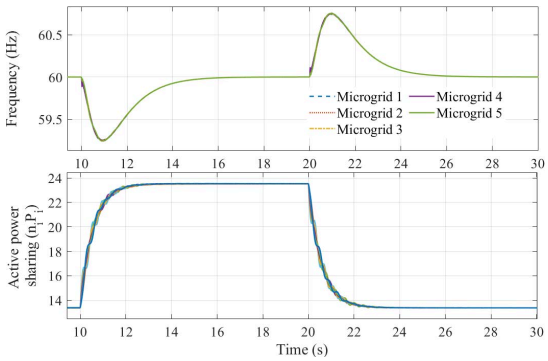

Fig. 4. DERs' frequencies throughout the network after attaching and detaching the step load.

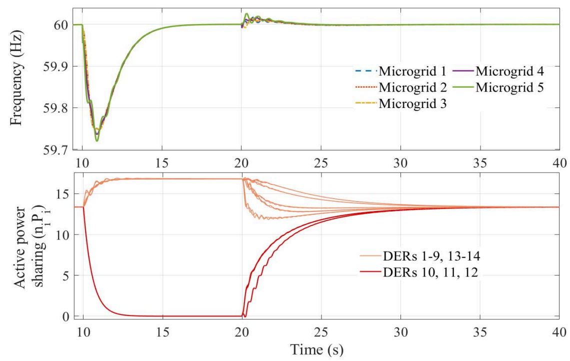

Fig. 5. Frequency regulation and active power sharing after plug-and-play of DERs 10, 11 and 12.

converges to the pinner as $t \to \infty$. Thus, $n_i P_i = \phi_i / k$ and $n_i P_i = n_j P_j \quad \forall i, j$ and ω_i converges to ω^*.

B. Verification on an AC Networked-Microgrid Case Study

The performance of the developed QDC is tested on a networked microgrids with five AC microgrids each one has 3 DERs (Fig. 3). The nominal voltage and frequency are 380 V and 60 Hz, respectively. For the sake of

simulation, two scenarios are examined. In the first scenario, the system is examined in the face of attaching and detaching a step load. To verify the QDC's feature of plug-and-play capability, as the second scenario, plug-and-play of DERs is tested. To simulate Eq. (3), the Python-based open source software QuTiP [13] is exploited.

1) Controller Performance: Studies in this section illustrate the performance of the QDC under a step load change of 40 kW applied to microgrid 2 at t = 10s and detached at t = 20s and results are depicted in Fig. 4. The exploited communication graph is shown in Fig. 3. As can be seen, frequency regulation is maintained throughout the step load changes and Active power is accurately shared among the heterogeneous participating DERs throughout the entire runtime.

2) Plug-and-play functionality: This case verifies the QDC's feature of plug-and-play capability. This merit is investigated, by detaching DER$_{10}$, DER$_{11}$ and DER$_{12}$ at t = 10s and plugging them in again at t = 20s. As depicted in Fig. 5, after disconnection of the DERs, the power deficiency reallocated among the remaining DERs and they manage to share the loads. As shown, accurate active power sharing and frequency restoration are maintained during plug-and-play operation.

C. Quantum Distributed Voltage Control for DC Microgrids.

In DC microgrids, droop control function is mainly utilized to provide decentralized power sharing. It generates the voltage reference V_i^{ref} as [14] $V_i^{\text{ref}} = V^* - m_i I_i$ where V^* is the nominal dc voltage, m_i is the current droop gain, I_i is the output current of DER$_i$. Consider the DC microgrid depicted in Fig. (6), ignoring the inductance effect of lines, the DC bus voltage V_b can be determined as $V_b = V_i^{\text{ref}} - R_i I_i$. It can be shown that, if the current droop gain m_i is set much larger than the line resistance R_i, $\frac{I_i}{I_j} \approx \frac{m_i}{m_j}$ and $V_b \approx V_i^{ref} \; \forall i, j$. The larger m_i is chosen, the more accurate power sharing can be obtained, however, larger m_i may cause the dc bus voltage V_b to deviate more from the nominal value V^*. Therefore, we aim to attain both power sharing and precise voltage restoration, simultaneously, by adding the QDC. To equip the DC microgrid with the QDC, the droop function is modified as

$$\begin{aligned} V_i^{ref} &= V^* - m_i I_i + \frac{\phi_i}{c}, \\ \dot{\phi}_i &= \sin\left(c m_i I_i - \phi_i\right) + \sum_{j=1}^{n} a_{i,j} \sin\left(\phi_j - \phi_i\right), \end{aligned} \tag{12}$$

Again, we select c such that $c < \frac{\pi/2}{\max(m_i I_i)}$. Obviously, the first part in the secondary control dynamic is to drive the dc bus voltage V_b to the nominal value V^* while the second part is to guarantee that $\phi_i = \phi_j$ is satisfied, i.e., the current sharing is achieved which demonstrates that the QDC is also applicable to distributed voltage control in DC microgrids.

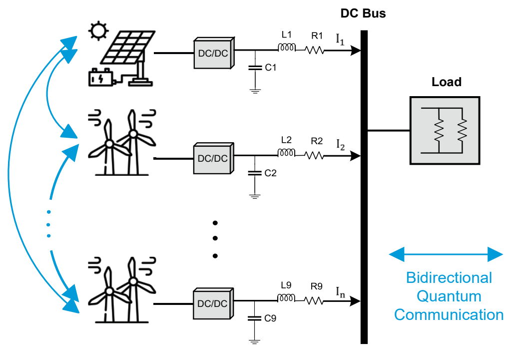

Parameter	Value
DC-Link Voltage	200 V
Filter Inductance	$L_1,\ L_2,\ L_5,\ L_6,\ L_7,\ L_9 = 5e^{-3}$ $L_3 = 4e^{-3}$ $L_4 = 4.5e^{-3}$ $L_8 = 5.5e^{-3}$
Filter Capacitance	$C_1,\ C_4,\ C_6,\ C_9 = 20e^{-6}$ $C_2,\ C_5,\ C_7 = 30e^{-6}$ $C_3,\ C_8 = 40e^{-6}$
Line Resistance	$R_1,\ R_3,\ R_7,\ R_9 = 0.02\ \Omega$ $R_4,\ R_6 = 0.015\Omega$, $R_5,\ R_8 = 0.025\ \Omega$ $R_2 = 0.01\ \Omega$
Droop Gain	$m_1 = 5e^{-3},\ m_2 = 4e^{-3},\ m_3 = 3e^{-3},$ $m_4 = 2e^{-3},\ m_5 = 1e^{-3},\ m_6 = 6e^{-3},$ $m_7 = 7e^{-3},\ m_8 = 8e^{-3},\ m_9 = 9e^{-3}$
Voltage Loop	$K_{VP} = 0.12,\ K_{VI} = 6$
Current Loop	$K_{IP} = 0.2,\ K_{II} = 1e^{-4}$
Load	$R_L = 0.15\ \Omega$

Fig. 6. DC microgrid model equipped with the QDC and parameters.

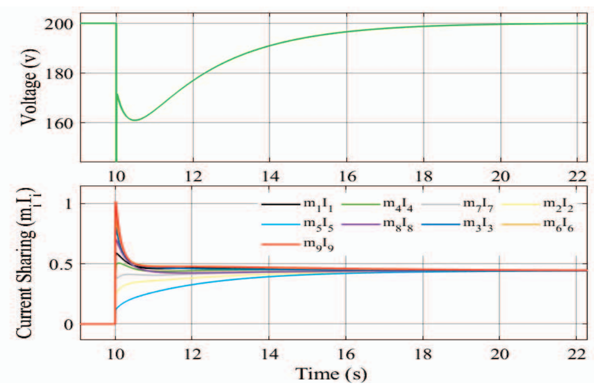

Fig. 7. Voltage regulation and current sharing after a step load disturbance at t = 10s.

D. Verification on a DC Microgrid Case Study.

This case verifies the universality of the QDC. This merit is investigated by equipping a 9 DER DC microgrid case study with the QDC (see Fig. 6) and applying a step load of 267 kw at t = 10s. Results are depicted in Fig. (7). The exploited communication graph is shown in Fig. (6). As can be seen, voltage regulation is guaranteed throughout the step load disturbance and power/current is accurately shared among the participating DERs throughout the runtime.

V. Conclusion

While we are on the verge of quantum internet, planning for future smart power grids, based on classical communications seems obsolete and may fail to address the new requirements and security challenges. Therefore, keeping up with the quantum technology seems essential. In this work we introduce a new synchronization mechanism by means of the quantum properties of qubits. We leverage a proposed master equation to construct the network of differential equations and demonstrate that the synchronization rule follows the forced Kuramoto model. We show how our proposed quantum synchronization scheme can be exploited to regulate AC microgrids' frequency and DC microgrids' voltage and guarantee precise power sharing.

Regarding the realization, the QDC requires establishing quantum communication among the nodes and having quantum computers at the nodes to simulate the master equation (3). On the quantum hardware side, there are some promising findings and developments. For example, right now, the 127-qubit Eagle processor is the largest IBM real quantum machine. However, according to the road map of IBM, a 1000-qubit Quantum machine, called Condor, will be available by the end of 2023 [15]. Developments like this are major steps toward commercializing quantum computers. On the computation side, authors in [16] have proposed a gate-based algorithm for simulating master equations and open quantum system dynamics on real quantum machines. This is another ongoing research direction, since new methods for decreasing quantum circuits depth are ever emerging.

References

[1] P. Babahajiani, L. Wang, J. Liu, and P. Zhang, "Push-sum-enabled resilient microgrid control," *IEEE trans. Smart Grid*, vol. 12, no. 4, pp. 3661–3664, 2021.

[2] L. Chen, D. Yue, C. Dou, J. Chen, and Z. Cheng, "Study on attack paths of cyber attack in cyber-physical power syst.s," *IET Generation, Transmission Distribution*, vol. 14, no. 12, pp. 2352–2360, 2020.

[3] Z. Tang, Y. Qin, Z. Jiang, W. O. Krawec, and P. Zhang, "Quantum-secure microgrid," *IEEE trans. Power Syst.s*, vol. 36, no. 2, pp. 1250–1263, 2021.

[4] D. Castelvecchi, "Quantum network is step towards ultrasecure internet," *Nature*, vol. 590, no. 7847, pp. 540–541, 2021.

[5] ——, "The quantum internet has arrived (and it hasn't)," *Nature*, vol. 554, no. 7690, pp. 289–293, 2018.

[6] G. Shi, D. Dong, I. R. Petersen, and K. H. Johansson, "Reaching a quantum consensus: Master equations that generate symmetrization and synchronization," *IEEE trans. Autom. Control*, vol. 61, no. 2, pp. 374–387, 2016.

[7] L. Mazzarella, A. Sarlette, and F. Ticozzi, "Consensus for quantum networks: Symmetry from gossip interactions," *IEEE trans. Autom. Control*, vol. 60, no. 1, pp. 158–172, 2015.

[8] M. A. Nielsen and I. L. Chuang, *Quantum Computation and Quantum Information: 10th Anniversary Edition*. Cambridge University Press, 2010.

[9] J. Preskill, "Lecture notes for physics: Quantum information and computation," 1998.

[10] H. M. Wiseman and G. J. Milburn, *Quantum measurement and control*. Cambridge university press, 2009.

[11] X. Lu, X. Yu, J. Lai, Y. Wang, and J. M. Guerrero, "A novel distributed secondary coordination control approach for islanded microgrids," *IEEE Trans. on Smart Grid*, vol. 9, no. 4, pp. 2726–2740, July 2018.

[12] M. Shi, X. Chen, M. Shahidehpour, Q. Zhou, and J. Wen, "Observer-based resilient integrated distributed control against cyberattacks on sensors and actuators in islanded ac microgrids," *IEEE trans. Smart Grid*, vol. 12, no. 3, pp. 1953–1963, 2021.

[13] J. Johansson, P. Nation, and F. Nori, "Qutip 2: A python framework for the dynamics of open quantum systems," *Computer Physics Communications*, vol. 184, no. 4, pp. 1234 – 1240, 2013.

[14] V. Nasirian, A. Davoudi, F. L. Lewis, and J. M. Guerrero, "Distributed adaptive droop control for dc distribution systems," *IEEE trans. Energy Conversion*, vol. 29, no. 4, pp. 944–956, 2014.

[15] E. National Academies of Sciences, Medicine *et al.*, *Quantum computing: progress and prospects*. National Academies Press, 2019.

[16] A. W. Schlimgen, K. Head-Marsden, L. M. Sager, P. Narang, and D. A. Mazziotti, "Quantum simulation of open quantum systems using a unitary decomposition of operators," *Physical Review Letters*, vol. 127, no. 27, p. 270503, 2021.

978-1-6654-0823-3/22/$31.00 ©2022 IEEE